Charge transport in chiral solids as a possible tool in search of dark matter signals

Marek Rogatko[*] and Karol I. Wysokinski[†]

Institute of Physics, Maria Curie-Sklodowska University, pl. Marii Curie-Sklodowskiej 1, 20-031 Lublin, Poland

(Received 7 June 2023; accepted 8 November 2023; published 28 November 2023)

As the existing techniques to directly detect dark matter particles in laboratory experiments continue to produce negative signals, the research community considers novel approaches including those relying on condensed matter systems with nontrivial quantum properties. For example, finding signatures of dark matter in transport characteristics of solids would be an important step on the road to detect this illusive component of the mass of our Universe. As a first step in this direction we have recently derived the modified kinetic equation taking into account two coupled $U(1)$-gauge fields, one being the standard Maxwell electromagnetic field and other corresponding to the dark sector. The resulting Boltzmann kinetic equation is modified by the Berry curvature which couples to both visible and dark sector gauge fields. The linear and nonlinear longitudinal and/or Hall currents in topological matter may signal the existence of dark particle induced electromagnetic fields. The usage of appropriately designed resonant cavity to enhance the electric field may help to reach the goal. The conservative estimates show that the technique should have the sensitivity of the order of 10^{-9} or better and may help to partially fill the gap between XENON1T and haloscope experiments.

DOI: 10.1103/PhysRevD.108.104062

I. INTRODUCTION

The only evidences of a dark matter [1] come from the gravitational observations. The signals include galaxy rotation curves, gravitational lensing and the gravitational structures at cosmological scales [2]. The search for this elusive, albeit dominant, component of the matter in our Universe by various techniques continues [3] to give negative effects. The direct unique signals of dark matter (DM) in the laboratory experiments would provide a breakthrough comparable to the first observation of the gravitational waves, which also resulted in the proposal that primordial black holes may in fact constitute the dark matter [4]. The absence of evidence for dark-matter particles despite extensive search results in a "sense of 'crisis' in the dark-matter particle community" [5]. Observing this state of the affairs the authors of [5] propose: "We argue that diversifying the experimental effort and incorporating astronomical surveys and gravitational wave observations is our best hope of making progress on the dark-matter problem". On the other hand, this situation provokes the appearance of novel detection techniques and theoretical models of dark matter.

The mass of DM particle is unknown and may span many orders of magnitude [6]. Some novel proposals consider dark matter candidates with huge masses as, e.g., the mentioned [4] primary black holes or the recently suggested fractionally charged gravitino with the mass at Planck scale [7]. Many of other recent proposals concentrate on the opposite end and consider relatively low masses in the eV range or even much below. The detection schemes of small-mass candidates are necessarily very different from the existing techniques.

Many of the new proposals are based on observations of condensed matter phenomena. It is condensed matter in which elementary excitations are observed at low energies and may be used as detectors of small-mass dark matter particles. Various novel methods have recently been discussed [8–23] proposing to use both, standard condensed matter systems and quantum materials, with a topologically nontrivial band structure. The latter include *inter alia* detecting DM with help of the superconducting materials [24–28] or superconducting qubits [9], graphene-based Josephson junctions [8], or by observing chiral magnetic effect in topologically nontrivial quantum matter [10,11].

Other detection techniques encompass the search for bosonic dark matter via absorption in superconductors [17], using superfluid helium [18], optical phonons in polar materials [19], observations of color center production in crystals [20], the usage of bulk three-dimensional Dirac semimetals [21] or multilayered optical devices [23]. The future will tell which of them turns out to be successful. The usage of various condensed matter systems and detection

[*]rogat@kft.umcs.lublin.pl
[†]karol@tytan.umcs.lublin.pl

techniques involving charge carriers; phonons, light, and quasiparticles in superconductors to detect light-dark matter has been recently reviewed [29,30].

The popular candidates for ultralight DM bosonic particles are axions (more generally axionlike particles) and dark photons. They manifest as a dark-electric (or magnetic) field oscillating with frequency $\tilde{\omega} = m_{\mathrm{DP}}c^2/\hbar$, where m_{DP} is the dark-particle mass, c denotes speed of light, and $\hbar$ is the reduced Planck constant. In this paper we concentrate on the massive dark photon as an important candidate.

Our starting point will be $(3+1)$-dimensional action describing the visible sector comprising Maxwell $U(1)$-gauge field and the hidden one with a massive $U(1)$-gauge auxiliary field $\tilde{A}_\mu$ (dark photon), interacting with the ordinary Maxwell field by the so-called kinetic mixing term. The action is provided by

$$S_{M\text{-dark photon}} = \int d^4x \left(-\frac{1}{4}F_{\mu\nu}F^{\mu\nu} - \frac{1}{4}\tilde{F}_{\mu\nu}\tilde{F}^{\mu\nu} - \frac{\alpha}{2}F_{\mu\nu}\tilde{F}^{\mu\nu} - \frac{m_{\mathrm{DP}}^2}{2}\tilde{A}_\mu\tilde{A}^\mu \right), \tag{1}$$

where α is a coupling constant between two sectors, standing in front of the kinetic mixing term. m_{DP} denotes here the mass of dark photon. $F_{\mu,\nu} = \partial_\mu A_\nu - \partial_\nu A_\mu$, and $\tilde{F}_{\mu,\nu} = \partial_\mu \tilde{A}_\nu - \partial_\nu \tilde{A}_\mu$ denote the field-strength tensors of the standard and dark photon, respectively. The coupling α is expected to be $\ll 1$.

The idea that dark photon can be a candidate for dark matter has been widely exploited on various backgrounds, both theoretically [31–36] and experimentally [37–42]. The model in question possesses also some possible astrophysical confirmations [43–47]. We have cited only some illustrative examples due to the vast amount of work authorizing this blossoming field of research.

Dark photons, the ultralight candidates for dark matter, interact with the Standard Model particles via the kinetic mixing term. After appropriate rotation and redefinitions, one can eliminate kinetic mixing term and arrive at the Lagrangian for dark photon, Maxwell field and electromagnetic current [48]. Thus, on the solid-state physics background we can say that dark photon interacts with electrons in solids. More generally, the scattering of dark particlelike axions (in the presence of external magnetic field) or dark photon produces small electric field oscillating with frequency $\tilde{\omega}$ at the surface of a metal or superconductor [49–51] and this can possibly be detected.

In a recent paper [10] we considered the chiral magnetic effect induced by dark photon in the Dirac semimetal. Chiral magnetic effect denotes the current flowing along the applied magnetic field in conducting material with a Berry curvature; in the mentioned paper the current flows along dark magnetic field $\tilde{\mathbf{B}}$. In that scenario the very existence of the signal relies on the kinetic coupling, which is a source of the dark magnetic field. The estimates show that the expected dark magnetic field is small and thus detection of the nondissipative current will be difficult, but not impossible. In contrast, the work [11] also proposing measurement of the chiral magnetic effect, assumes application of the external magnetic field and detection of axionlike particles. In that work the current flows along the direction of the external magnetic field $\mathbf{B}$.

In the present paper, we extend our previous work and consider detection of dark matter via measurement of anomalous transport in Dirac or Weyl semimetals [52,53], with broken time-reversal or inversion symmetry. Dirac or Weyl semimetals are three or two-dimensional condensed matter systems with topologically nontrivial energy spectrum, which is characterized by the existence of Dirac nodes and zero, or very small energy gap between conduction and valence bands. The oscillating electric field induced by dark particles like axions or dark photons in a two-dimensional Weyl or Dirac semimetals, could be identified by observing in a such systems two kinds of electric currents flowing in mutually perpendicular directions, i.e., the longitudinal and anomalous Hall current. The latter appears at linear electric-field order if the time-reversal symmetry is broken. On the other hand, at higher order in electric field strength, the anomalous Hall effect appears even when the Hamiltonian is time-reversal invariant, but other symmetries like inversion are broken [54]. Two-dimensional transition metal dichalcogenides [55,56] or three-dimensional Weyl semimetals [52] could serve as potential candidates to observe the effect and thus as detectors of dark matter fields.

The organization of the rest of the paper is as follows. In Sec. II we briefly recall the Boltzmann kinetic theory application to chiral systems, like Weyl or Dirac semimetals in the Maxwell $\mathbf{E}$ and dark-sector $\tilde{\mathbf{E}}$ electric fields. We solve the Boltzmann equation in Sec. III. The currents in the system with two electric fields are calculated in Sec. IV. The estimation of the dark particle induced electric field is a subject of Sec. V, while its possible enhancement in a resonant cavity is discussed in Sec. VI. The estimates of the sensitivity of the proposed measurements are presented in Sec. VII. We conclude with a discussion of a few scenarios to identify signal of dark matter in Sec. VIII.

II. BOLTZMANN KINETIC EQUATION FOR SYSTEMS WITH BERRY CURVATURE AND DARK MATTER

Standard Boltzmann kinetic theory applied to Weyl and Dirac systems requires a modification which takes into account the existence of the Berry curvature $\mathbf{\Omega}(\mathbf{k})$, in such materials. The existence of a nontrivial electron spectrum and resulting Berry curvature is known to modify the equations of motion of the electron velocity $\dot{\mathbf{r}}$ and momentum $\dot{\mathbf{k}}$, as well as a phase-space volume $d\mathbf{r}d\mathbf{k}$ [57]. Strictly speaking, the Boltzmann kinetic equation has its

standard form. However, the velocity of a particle is modified by the presence of Berry curvature and this induces the modification of the particles' dynamics.

On the other hand, the Boltzmann equation allows one to find the local distribution function [58] $f(r,\mathbf{k},t)$ in the presence of external perturbations. In Weyl or Dirac semimetals with nodes of different chirality, the distribution may depend on the node in question. Thus, in general we denote the distribution around the node c by $f_c(\mathbf{r},\mathbf{k},t)$. It changes in time according to the relation

$$\frac{\partial f_c(\mathbf{r},\mathbf{k},t)}{\partial t}+\dot{\mathbf{r}}_c\cdot\boldsymbol{\nabla}_{\mathbf{r}}f_c(\mathbf{r},\mathbf{k},t)+\dot{\mathbf{k}}_c\cdot\boldsymbol{\nabla}_{\mathbf{k}}f_c(\mathbf{r},\mathbf{k},t) = I_{\mathrm{coll}}[f_c(\mathbf{r},\mathbf{k},t)]. \tag{2}$$

Here $I_{\mathrm{coll}}[f_c(\mathbf{r},\mathbf{k},t)]$ is the collision integral.

In systems with Berry phase the time dependence of $\mathbf{r}$ and $\mathbf{k}$ near the node c is found [57,59] and is provided by

$$\dot{\mathbf{r}}_c=\frac{1}{D_c(\mathbf{k})}\left[\mathbf{v}_c+\frac{e}{\hbar}(\mathbf{v}_c\cdot\boldsymbol{\Omega}_c)\mathbf{B}+\frac{e}{\hbar}(\mathbf{E}\times\boldsymbol{\Omega}_c)\right], \tag{3}$$

$$\hbar\dot{\mathbf{k}}_c=\frac{1}{D_c(\mathbf{k})}\left[-e\mathbf{E}-e\mathbf{v}_c\times\mathbf{B}-\frac{e^2}{\hbar}(\mathbf{E}\cdot\mathbf{B})\boldsymbol{\Omega}_c\right]. \tag{4}$$

In the above equation $\boldsymbol{\Omega}_c$ denotes the wave-vector dependent Berry curvature $\boldsymbol{\Omega}_c(\mathbf{k})$ at node c and $D_c(\mathbf{k})=1+\frac{e}{\hbar}(\mathbf{B}\cdot\boldsymbol{\Omega}_c)$ is the phase-space correction factor [57].

Our interest is focused on the solution of Boltzmann equation which simplifies considerably in homogeneous systems and in the absence of external magnetic field [54,60,61]. With such an assumptions of system homogeneity and absence of magnetic field, the distribution function $f(r,\mathbf{k},t)=f(\mathbf{k},t)$ is independent on $\mathbf{r}$. We suppose also the validity of the relaxation-time approximation. The Boltzmann equation reduces to

$$\frac{\partial f(\mathbf{k},t)}{\partial t}+\dot{k}^a\frac{\partial f(\mathbf{k},t)}{\partial k_a}=-\frac{f(\mathbf{k},t)-f_0(\mathbf{k},0)}{\tau}. \tag{5}$$

For simplicity, we neglect here the explicit dependence on c and assume the relaxation time τ is isotropic and constant.

In the model with standard electric field $E^a(t)=\mathrm{Re}(E_0^a e^{i\omega t})$ and dark matter electric field $\tilde{E}^a(t)=\mathrm{Re}(\tilde{E}_0^a e^{i\tilde{\omega}t})$, the electron charge $(-e)$ changes its momentum as a result of the electric force [10]

$$\hbar\dot{k}^a=-e\left[E^a(t)+\frac{\alpha}{2}\tilde{E}^a(t)\right]=-e\,\mathrm{Re}\left(E_0^a e^{i\omega t}+\frac{\alpha}{2}\tilde{E}_0^a e^{i\tilde{\omega}t}\right), \tag{6}$$

where α is the coupling constant in the kinetic mixing between two $U(1)$-gauge fields in Eq. (1). It is a source of the change of the total electric field acting upon an electron in the background of dark matter sector.

III. SOLUTION OF THE BOLTZMANN EQUATION IN THE PRESENCE OF MAXWELL AND DARK MATTER FIELDS

This section is devoted to the solution of Eq. (5). We shall find corrections to the distribution function to an arbitrary order in the electric fields $\mathbf{E}(t)$ and $\tilde{\mathbf{E}}(t)$. For a standard Maxwell electric field only, the solutions can be found in Refs. [54,60,61]. Even though it is possible to generalize the previous work [60] and obtain the nonperturbative solution of Eq. (5) we limit the discussion to quadratic order. To this end, in this section we follow Zhang *et al.* [61].

To commence with, one writes the total distribution function as a sum given by

$$f(\mathbf{k},t)=\mathrm{Re}(f_0+f_1+f_2+\cdots f_n+\cdots), \tag{7}$$

where f_n is assumed to vanish as a power $E_0^n,\tilde{E}_0^n$. Keeping in mind the relations (5)–(6) and counting the powers of electric fields, we derive the set of equations

$$\tau\partial_t f_0(\mathbf{k},t)=0, \tag{8}$$

$$\tau\partial_t f_1+f_1=\frac{e\tau}{2\hbar}\left(E_0^a e^{i\omega t}+E_0^{*a}e^{-i\omega t}+\frac{\alpha}{2}\tilde{E}_0^a e^{i\tilde{\omega}t}+\frac{\alpha}{2}\tilde{E}_0^{*a}e^{-i\tilde{\omega}t}\right)\partial_a f_0, \tag{9}$$

$$\tau\partial_t f_2+f_2=\frac{e\tau}{2\hbar}\left(E_0^a e^{i\omega t}+E_0^{*a}e^{-i\omega t}+\frac{\alpha}{2}\tilde{E}_0^a e^{i\tilde{\omega}t}+\frac{\alpha}{2}\tilde{E}_0^{*a}e^{-i\tilde{\omega}t}\right)\partial_a f_1, \quad \cdots, \tag{10}$$

$$\tau\partial_t f_n+f_n=\frac{e\tau}{2\hbar}\left(E_0^a e^{i\omega t}+E_0^{*a}e^{-i\omega t}+\frac{\alpha}{2}\tilde{E}_0^a e^{i\tilde{\omega}t}+\frac{\alpha}{2}\tilde{E}_0^{*a}e^{-i\tilde{\omega}t}\right)\partial_a f_{n-1}, \quad \text{etc.} \tag{11}$$

We have used here the shorthand notations $\partial_t = \frac{\partial}{\partial t}$ and $\partial_a = \frac{\partial}{\partial k_a}$. The above equations can be solved order by order.

Equation (8) comprises a statement such that the equilibrium distribution function does not depend on time $f_0(\mathbf{k}, t) = f_0(\mathbf{k})$. Further, one assumes that the initial distribution is given by the Fermi-Dirac function corresponding to temperature T and chemical potential μ. Namely, we have

$$f_0(\mathbf{k}) = \frac{1}{e^{\frac{\varepsilon(\mathbf{k})-\mu}{k_B T}} + 1}. \tag{12}$$

The solution of Eq. (9) is simple and can be written as

$$f_1(\mathbf{k}, t) = \mathrm{Re}(f_1^{\omega} e^{i\omega t} + f_1^{\tilde{\omega}} e^{i\tilde{\omega} t}), \tag{13}$$

where we have denoted

$$f_1^{\omega} = \frac{e\tau}{\hbar} \frac{E_0^a \partial_a f_0}{(1 + i\omega\tau)}, \tag{14}$$

$$f_1^{\tilde{\omega}} = \frac{\alpha}{2} \frac{e\tau}{\hbar} \frac{\tilde{E}_0^a \partial_a f_0}{(1 + i\tilde{\omega}\tau)}. \tag{15}$$

The second-order term $f_2(\mathbf{k}, t)$, for two oscillating fields, introduces various harmonic functions with frequencies $2\omega, 2\tilde{\omega}, \omega \pm \tilde{\omega}$. Interestingly, the frequency-independent term also contributes at the second order. After some algebra one arrives at the relation

$$\begin{aligned} f_2(\mathbf{k}, t) = \mathrm{Re}(&f_2^{(0)} + f_2^{(2\omega)} e^{2i\omega t} + f_2^{(2\tilde{\omega})} e^{2i\tilde{\omega} t} \\ &+ f_2^{(\omega+\tilde{\omega})} e^{i(\omega+\tilde{\omega})t} + f_2^{(\omega-\tilde{\omega})} e^{i(\omega-\tilde{\omega})t}), \end{aligned} \tag{16}$$

where the frequency dependent coefficients imply

$$f_2^{(0)} = \left(\frac{e\tau}{\hbar}\right)^2 \left[\frac{E_0^{*b} E_0^a \partial_{ab} f_0}{2(1 + i\omega\tau)} + \left(\frac{\alpha}{2}\right)^2 \frac{\tilde{E}_0^{*b} \tilde{E}_0^a \partial_{ab} f_0}{2(1 + i\tilde{\omega}\tau)}\right], \tag{17}$$

$$f_2^{(2\omega)} = \left(\frac{e\tau}{\hbar}\right)^2 \frac{E_0^b E_0^a \partial_{ab} f_0}{2(1 + i\omega\tau)(1 + 2i\omega\tau)}, \tag{18}$$

$$f_2^{(2\tilde{\omega})} = \alpha^2 \left(\frac{e\tau}{2\hbar}\right)^2 \frac{\tilde{E}_0^b \tilde{E}_0^a \partial_{ab} f_0}{2(1 + i\tilde{\omega}\tau)(1 + 2i\tilde{\omega}\tau)}, \tag{19}$$

$$\begin{aligned} f_2^{(\omega+\tilde{\omega})} = \alpha \left(\frac{e\tau}{2\hbar}\right)^2 &\left[\frac{E_0^b \tilde{E}_0^a \partial_{ab} f_0}{(1 + i\tilde{\omega}\tau)} + \frac{\tilde{E}_0^b E_0^a \partial_{ab} f_0}{(1 + i\omega\tau)}\right] \\ &\times \frac{1}{[1 + i(\omega + \tilde{\omega})\tau]}, \end{aligned} \tag{20}$$

$$\begin{aligned} f_2^{(\omega-\tilde{\omega})} = \alpha \left(\frac{e\tau}{2\hbar}\right)^2 &\left[\frac{E_0^b \tilde{E}_0^{*a} \partial_{ab} f_0}{(1 - i\tilde{\omega}\tau)} + \frac{\tilde{E}_0^{*b} E_0^a \partial_{ab} f_0}{(1 + i\omega\tau)}\right] \\ &\times \frac{1}{[1 + i(\omega - \tilde{\omega})\tau]}. \end{aligned} \tag{21}$$

The higher-order corrections can be obtained in a similar way, if needed. In the next section we use the above formulas to calculate the ac currents in the chiral system.

IV. CURRENTS IN CHIRAL SYSTEMS AFFECTED BY THE DARK FIELD

We are mainly interested in detecting dark matter fields which may arise in the rare scattering processes of dark particles with ordinary matter particles. For this purpose, we analyse the currents flowing in general systems, i.e., those with and without Berry curvature and only later we discuss possible detection scenarios. For chiral systems the velocity, the distribution function and the Berry curvature, depend on the node index c. However, in the following formulas we neglect this dependence and restrict our attention to the discussion of the currents to the second order in the field strength. To find the total current one has to take all nodes existing in a given material.

In the kinetic equation approach the current flowing in d-dimensional system is calculated from the relation

$$j^a(t) = -e \int \frac{d^d k}{(2\pi)^d} \dot{r}^a f(\mathbf{k}, t), \tag{22}$$

and can be found to an arbitrary order in electric field. However, in a chiral system influenced by the dark matter sector, the velocity $\dot{\mathbf{r}}$ is modified by the Berry curvature and dark electric field [10]

$$\dot{r}^a = v^a(\mathbf{k}) - \frac{e}{\hbar} \epsilon^{abc} \Omega_b(\mathbf{k}) \left(E_c(t) + \frac{\alpha}{2} \tilde{E}_c(t)\right). \tag{23}$$

In the linear (in electric fields) order, the longitudinal currents flow whatever the symmetry of the crystal, however the existence of the Hall effect requires breaking the time-reversal symmetry. In the nonlinear regime the Hall current can be measured even in time-reversal symmetric systems. It appears at second [54] or higher [61–64] orders in the electric field.

We calculate the current from the relation (22), with the usage of Eq. (23), first expanding the distribution function with respect to powers of electric fields, as given in (7) and (6). To the lowest order, i.e., using $f(\mathbf{k}, t) = \mathrm{Re}(f_0)$, one obtains

$$\begin{aligned} j_0^a(t) = -e \int \frac{d^d k}{(2\pi)^d} &\left[v^a(\mathbf{k}) \right. \\ &\left. - \frac{e}{\hbar} \epsilon^{abc} \Omega_b \mathrm{Re}\left(E_c(t) + \frac{\alpha}{2} \tilde{E}_c(t)\right)\right] f_0(\mathbf{k}). \end{aligned} \tag{24}$$

This can be rewritten as follows:

$$j_0^a(t) = \mathrm{Re}(j_0^a + j_0^{a(\omega)} e^{i\omega t} + j_0^{a(\tilde{\omega})} e^{i\tilde{\omega} t}), \tag{25}$$

where we have denoted

$$j_0^{a(0)} = -e\int \frac{d^dk}{(2\pi)^d} v^a(\mathbf{k}) f_0(\mathbf{k}), \tag{26}$$

$$j_0^{a(\omega)} = \frac{e^2}{\hbar}\int \frac{d^dk}{(2\pi)^d} \epsilon^{abc}\Omega_b E_{(0)c} f_0(\mathbf{k}), \tag{27}$$

$$j_0^{a(\tilde{\omega})} = \frac{\alpha}{2}\frac{e^2}{\hbar}\int \frac{d^dk}{(2\pi)^d} \epsilon^{abc}\Omega_b \tilde{E}_{(0)c} f_0(\mathbf{k}). \tag{28}$$

The total current related to the unperturbed distribution function f_0 consists of three terms. The first of them is proportional to the velocity $v^\alpha(\mathbf{k})$ and is independent of the electric field. This rectified current $j_0^{a(0)}$ is purely classical. Its existence does not require Berry curvature. However, it vanishes due to the fact that velocity is an odd function of momentum $v^a(\mathbf{k}) = -v^a(-\mathbf{k})$. This is correct, as there can not be a current flow in the equilibrium.

On the other hand, the anomalous velocity induced by the Berry curvature [second term in Eq. (23)] also gives the currents proportional to the unperturbed distribution function and to the electric field. To the first order in the field, the current possesses two harmonic contributions bounded with the standard and dark field of frequency ω and $\tilde{\omega}$, respectively. It is this second contribution, that appearance signals the dark sector effect. This is true, even in the experimental setup with $\omega = 0$, i.e., for the static standard electric field $E^a(t) = E_0^a$.

For $f(\mathbf{k}, t)$ linear in both fields [$f_1(\mathbf{k}, t)$], one finds the current, which contains linear and quadratic terms in electric fields. The linear terms result from the velocity $\mathbf{v}$, while quadratic ones are due to $\mathbf{E}\times\mathbf{\Omega}$ term in relation (23). Thus, we obtain the total time dependent current consisting of various components, each oscillating at a specific frequency

$$\begin{aligned} j_1^a(t) = \mathrm{Re}(&j_1^{a(0)} + j_1^{a(\omega)}e^{i\omega t} + j_1^{a(\tilde{\omega})}e^{i\tilde{\omega}t} + j_1^{a(2\omega)}e^{2i\omega t} \\ &+ j_1^{a(2\tilde{\omega})}e^{2i\tilde{\omega}t} + j_1^{a(\omega+\tilde{\omega})}e^{i(\omega+\tilde{\omega})t} + j_1^{a(\omega-\tilde{\omega})}e^{i(\omega-\tilde{\omega})t}), \end{aligned} \tag{29}$$

where the various coefficients are given by the following formulas:

$$j_1^{a(0)} = \frac{e^2}{2\hbar}\int \frac{d^dk}{(2\pi)^d} \epsilon^{abc}\Omega_b \left[E_{(0)c} f_1^{*(\omega)} + \frac{\alpha}{2}\tilde{E}_{(0)c} f_1^{*(\tilde{\omega})}\right], \tag{30}$$

$$j_1^{a(\omega)} = -e\int \frac{d^dk}{(2\pi)^d} v^a(\mathbf{k}) f_1^{(\omega)}, \tag{31}$$

$$j_1^{a(\tilde{\omega})} = -e\int \frac{d^dk}{(2\pi)^d} v^a(\mathbf{k}) f_1^{(\tilde{\omega})}, \tag{32}$$

$$j_1^{a(2\omega)} = \frac{e^2}{2\hbar}\int \frac{d^dk}{(2\pi)^d} \epsilon^{abc}\Omega_b E_{(0)c} f_1^{(\omega)}, \tag{33}$$

$$j_1^{a(2\tilde{\omega})} = \frac{\alpha}{2}\frac{e^2}{2\hbar}\int \frac{d^dk}{(2\pi)^d} \epsilon^{abc}\Omega_b \tilde{E}_{(0)c} f_1^{(\tilde{\omega})}, \tag{34}$$

$$j_1^{a(\omega+\tilde{\omega})} = \frac{e^2}{2\hbar}\int \frac{d^dk}{(2\pi)^d} \epsilon^{abc}\Omega_b \left[E_{(0)c} f_1^{(\tilde{\omega})} + \frac{\alpha}{2}\tilde{E}_{(0)c} f_1^{(\omega)}\right], \tag{35}$$

$$j_1^{a(\omega-\tilde{\omega})} = \frac{e^2}{2\hbar}\int \frac{d^dk}{(2\pi)^d} \epsilon^{abc}\Omega_b \left[E_{(0)c} f_1^{*(\tilde{\omega})} + \frac{\alpha}{2}\tilde{E}^*_{(0)c} f_1^{(\omega)}\right], \tag{36}$$

with $f_1^{(\omega)}$ and $f_1^{(\tilde{\omega})}$ given by Eqs. (14) and (15). Note, that the latter function contains the factor $\frac{\alpha}{2}$, which makes both coefficients (35) and (36) to be linear in the coupling constant α.

V. ESTIMATION OF THE DARK PHOTON INDUCED ELECTRIC FIELD

The very recent measurements of the local dark matter densities conducted by LAMOST DR5 and Gaia DR2 experiments [65,66], reveal that our Galactic disc is immersed in dark matter halo with a characteristic mass density $\rho_{\mathrm{DM}} = 0.5\ \mathrm{GeV/cm^3}$. In addition, the latest observations of the gravitational lensing seem to indicate that the model of wavelike dark matter better fits the observed lensing features (brightnesses and positions of multiple-lensed images), then the model of particlelike dark matter [67].

The dark matter density is expected to be bounded with the amplitude of the dark photon, and time and space components of its vector potentials $\tilde{A}^0$ and $\tilde{\mathbf{A}}$, which are subject to time and space dependences [51]

$$\tilde{A}^0(\mathbf{r}, t) = -\tilde{\mathbf{v}}\cdot\tilde{\mathbf{A}}_c\ \cos(m_{\mathrm{DP}}t - m_{\mathrm{DP}}\mathbf{v}\cdot\mathbf{r}), \tag{37}$$

$$\tilde{\mathbf{A}}(\mathbf{r}, t) = \tilde{\mathbf{A}}_c\ \cos(m_{\mathrm{DP}}t - m_{\mathrm{DP}}\mathbf{v}\cdot\mathbf{r}). \tag{38}$$

Furthermore, the time component of the dark photon field is suppressed by the velocity of dark sector around the Earth $|\mathbf{v}| \approx 10^{-3}c$. The field oscillates with frequency m_{DP} and thus provides a window for its detection by frequency dependent measurements. The amplitude $\tilde{\mathbf{A}}_c$ is related to the density of the dark matter ρ_{DM}, depending on the dark photon mass [49–51,68]

$$\rho_{\mathrm{DM}} = \frac{1}{2}m_{\mathrm{DP}}^2\tilde{\mathbf{A}}_c^2. \tag{39}$$

The dark photon induced electric field $\mathbf{E}$ at the surface of the metal with conductivity σ implies [51]

$$\mathbf{E} = \alpha\sqrt{\frac{m_{\mathrm{DP}}}{2\sigma}}\tilde{\mathbf{A}}_c[\cos(m_{\mathrm{DP}}t) - \sin(m_{\mathrm{DP}}t)]$$
$$= \alpha\sqrt{\frac{m_{\mathrm{DP}}}{\sigma}}\tilde{\mathbf{A}}_c\cos\left(m_{\mathrm{DP}}t + \frac{\pi}{4}\right). \tag{40}$$

The dark photon-induced electric field oscillates with frequency $\tilde{\omega} = \frac{m_{\mathrm{DP}}c^2}{\hbar}$ and is phase shifted by $\pi/4$, in comparison to the behavior assumed in Sec. II.

Combining (39) and (40) one finds the magnitude of the dark matter induced electric field amplitude

$$\tilde{\mathbf{E}}_0 = c\sqrt{2\mu_0\rho_{\mathrm{DM}}}, \tag{41}$$

in standard units. Using dark matter density 0.5 GeV/cm^3 we get $\tilde{\mathbf{E}}_0 \approx 130\frac{V}{m}$. This field oscillates at frequency in GHz regime, induces in vacuum the electric field, oscillating with the same frequency and small magnitude. Namely, one has

$$\mathbf{E}_0 = \alpha\tilde{\mathbf{E}}_0, \tag{42}$$

as discussed earlier.

VI. ENHANCING THE INDUCED FIELD

The induced electric field is scaled down by the kinetic mixing term $\propto$ coupling. Due to the fact that $\alpha \ll 1$ it would be of great importance to amplify its value. One possibility is to implement the cavity resonators. In such devices the electric field is reflected from two parallel mirrors distance L apart from each other. The wave moving towards one the mirrors is reflected back changing the sign of the wave vector and the sign of the amplitude. The appropriate boundary conditions require the vanishing of the field component parallel to the mirror. Depending on the details of the setup the electric field inside the resonator may be further increased.

The reflection process is always related to some losses of the signal. However, for the high-quality factor Q of the resonator the reflection coefficient r is close to unity. This is because [69]

$$r = 1 - \frac{\pi}{2Q}. \tag{43}$$

In typical resonators the standing waves form and this results in a very inhomogeneous electromagnetic fields. The field inhomogeneity makes standard resonators not applicable for the purpose of transport measurements and more complicated systems are needed. This can be achieved by supplementing the resonators with tuners (metallic reflectors) which change the boundary conditions and may give more homogeneous fields, at the expense that not all frequencies can be effectively used. With large quality factors one may get a resonator of arbitrary size and working frequency. The details depend on the size, shape, and construction of tuners. Smaller resonators allow for larger usable frequencies. Such devices are usually called electromagnetic reverberation chambers [70]. It is a complicated task to calculate the electric field enhancement in a resonator of arbitrary shape.

However, the order of magnitude estimation may be obtained by considering the simplest possible device consisting of two parallel metallic mirrors similar to that considered in [69]. It has been shown that both the external electric field $\mathbf{E}$ and the dark matter introduced field $\tilde{\mathbf{E}}$ get enhanced. The idea is as follows. Consider a resonator in a form of parallelepiped with two mirrors characterized by the reflection coefficient r. The electric field propagating with a wave vector $\mathbf{k}$ and frequency ω as a plane wave $\mathbf{E} = \mathrm{Re}[\mathbf{E}_0 e^{i(\mathbf{k}\cdot\mathbf{r}-\omega t)}]$, with the amplitude $\mathbf{E}_0$, is reflected back on the mirror with probability r changing the direction and wave vector to opposite one. During its travel from one mirror to another it also gets additional phase e^{ikL}, where k is component of $\mathbf{k}$ along the direction between the mirrors. After many such reflections, the resulting total field $\mathbf{E}_{\mathrm{tot}}(t)$ at $x = 0$, which is taken to be in the middle of the cavity, is found to be [69]

$$\mathbf{E}_{\mathrm{tot}}(t) = \mathrm{Re}\left[\mathbf{E}_0\frac{e^{i\frac{kL}{2}}}{1 + re^{ikL}}e^{-i\omega t}\right]. \tag{44}$$

Comparing this relation with our definition of the field amplitude given before Eq. (6), one notices that the factor

$$\mathbf{E}_{0\mathrm{tot}} = \mathbf{E}_0\frac{e^{i\frac{kL}{2}}}{1 + re^{ikL}}, \tag{45}$$

plays a role of $\mathbf{E}_0^*$, used previously. Thus for an experiment utilizing cavity one replaces everywhere in the previous formulas $\mathbf{E}_0$ by $\mathbf{E}_{0\mathrm{tot}}^*$.

As far as the dark matter field is concerned, we have to notice that according to the observations, it exists everywhere in the space around the Earth, moving with relative velocity $v \approx 10^{-3}c$ and is considered as a coherent over typical experimental distances. This leads to the conclusion that it produces the electric field $\alpha\tilde{\mathbf{E}}$ in both mirrors. However, only the component perpendicular to the mirrors, denoted $\tilde{\mathbf{E}}_\perp$, propagates and in effect only this component is enhanced. Adding the constant in space component one finds that the total dark matter field inside the cavity at $x = 0$, is given by [69]

$$\tilde{\mathbf{E}}_{\mathrm{tot}}(t) = \left[\tilde{\mathbf{E}}_0 + 2\tilde{\mathbf{E}}_{0\perp}\frac{e^{i\frac{kL}{2}}}{1 + re^{ikL}}\right]e^{-i\tilde{\omega}t}. \tag{46}$$

Once again we notice that the role of a complex amplitude of the dark matter field $\tilde{\mathbf{E}}_0^*$, used previously, is played by the following relation:

$$\tilde{\mathbf{E}}_{0\mathrm{tot}} = \left[\tilde{\mathbf{E}}_0 + 2\tilde{\mathbf{E}}_{0\perp}\frac{e^{i\frac{\tilde{k}L}{2}}}{1+re^{i\tilde{k}L}}\right], \tag{47}$$

where the frequency and the wave vector of dark matter massive field in the laboratory frame is calculated (for arbitrary boost direction) from

$$\frac{\tilde{\omega}'}{c} = \gamma\left(\frac{\omega}{c} - \mathbf{v}\cdot\mathbf{k}\right) \approx \frac{\omega}{c}, \tag{48}$$

$$\tilde{\mathbf{k}}' = \tilde{\mathbf{k}} + \frac{1}{v^2}(\gamma-1)(\tilde{\mathbf{k}}\cdot\mathbf{v})\mathbf{v} - \gamma\frac{\omega\mathbf{v}}{c^2}, \tag{49}$$

where $\gamma = 1/\sqrt{1-\frac{v^2}{c^2}}$. The approximate equality in the first equation is motivated by the fact that $\gamma \approx 1$. Similarly, this shows that $\tilde{\mathbf{k}}' \approx -\frac{\omega\mathbf{v}}{c^2}$, for the dark photon mode of interest, $\tilde{\mathbf{k}} = 0$. The wave vector $\tilde{\mathbf{k}}'$ can be neglected for macroscopic resonators, when $\tilde{k}'L \ll 2\pi$. The massless photon moves with $k = \frac{\omega}{c}$.

To proceed, we rewrite (45) and (47) in terms of photon frequencies as

$$\mathbf{E}_{0\mathrm{tot}} = \mathbf{E}_0\frac{e^{i\frac{\omega L}{2c}}}{1+re^{i\frac{\omega L}{c}}} = \mathbf{E}_0 B(\omega), \tag{50}$$

$$\tilde{\mathbf{E}}_{0\mathrm{tot}} = \tilde{\mathbf{E}}_0\left[1+2\beta\frac{e^{i\frac{\tilde{\omega}L}{2c}}}{1+re^{i\frac{\tilde{\omega}L}{c}}}\right] = \tilde{\mathbf{E}}_0 A(\tilde{\omega}), \tag{51}$$

and the parameter $\beta = 1/\sqrt{3}$ characterises the average value of the projection of dark photon field on the unit vector $\hat{\mathbf{n}}$ perpendicular to the mirror [69]. The frequency dependent factors $A(\tilde{\omega})$ and $B(\omega)$ provide the appropriate complex amplification amplitudes.

According to the previous discussion the transport experiments aimed at the discovery of dark matter will concentrate on the currents related to dark photon induced electric field. These include the anomalous Hall current (28), which existence does not require external field. Its value is enhanced by the amplitude $A(\tilde{\omega})$. Similarly, the longitudinal current (32), which also does not require external field is amplified by the same factor. The remaining two currents which are of linear order in α, namely relations (35) and (36) can be rewritten in terms of bar amplitudes and enhancement factors. One finds that the current depending on the sum of frequencies is enhanced by $A^*(\tilde{\omega})B^*(\omega)$, while that corresponding to the difference of frequencies is enhanced by the complex amplitude given by $A(\tilde{\omega})B^*(\omega)$. These enhancement factors are complex and their maximal values depend on the reflection coefficient r. For cavities with large Q values r is very close to 1 and the amplification factor may, for particular frequencies, attain very large values.

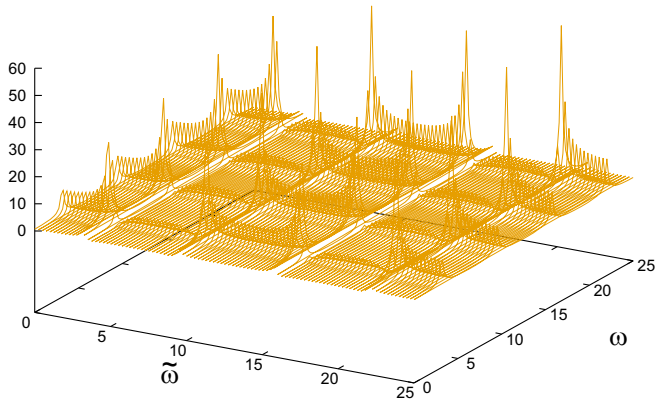

FIG. 1. The dependence of the modulus of amplification factor $W(\tilde{\omega},\omega) = A(\tilde{\omega})B^*(\omega)$ of the $\mathbf{j}_1^{\omega-\tilde{\omega}}$ current defined in Eq. (36). We measure frequencies in unit of c/L and assume the modest value of the reflection coefficient $r = 0.95$.

For the illustration purposes we use $r = 0.95$ and calculate the enhancement as a function of frequency ω and $\tilde{\omega}$, in units of c/L. In the Fig. 1 we plot the absolute value of the amplification factor $W(\tilde{\omega},\omega) = A(\tilde{\omega})B^*(\omega)$ which enters the current $\mathbf{j}_1^{\omega-\tilde{\omega}}$ defined by the relation (36). The amplification factor is large and gets larger with the increase of the r value. For $r = 0.999$ it reaches the value as large as a few thousands.

VII. SENSITIVITY ANALYSIS

As discussed in previous sections, at the linear order in the coupling α, the signals from dark photon of frequency $\tilde{\omega}$ which we expect to detect by using external high frequency ω radiation may appear at the set $\{\tilde{\omega}, \omega+\tilde{\omega}, \omega-\tilde{\omega}\}$ of frequencies. The signal at frequency $\tilde{\omega}$ appears at the linear order of the field $\tilde{\mathbf{E}}$, while the other at the second order of fields. As visible from the Eqs. (33), (35), and (36) the signals are proportional to $\tilde{\mathbf{E}}$ in the linear case and the combinations of the fields $\tilde{\mathbf{E}}\mathbf{E}$ enter the high-frequency anomalous nonlinear Hall signals. It has to be mentioned that high-frequency transport measurements of the longitudinal and Hall currents can utilize various techniques. The analysis of the projected experimental sensitivity may depend on the particular measurement technique. Here we concentrate on one source of experimental uncertainty which is the fluctuations in the amplitude of the field. The estimate of the limit on the coupling α due to this source are analogous to those in Ref. [69] and we shall follow their analysis.

The anomalous Hall currents we are interested in are of linear order in α and proportional to the products of two fields. For the measurements in the cavity one has to note that the cavity enhances both the field and its fluctuations. The latter are related to the power fed into the cavity and to the power fluctuations. Modeling the injected-field

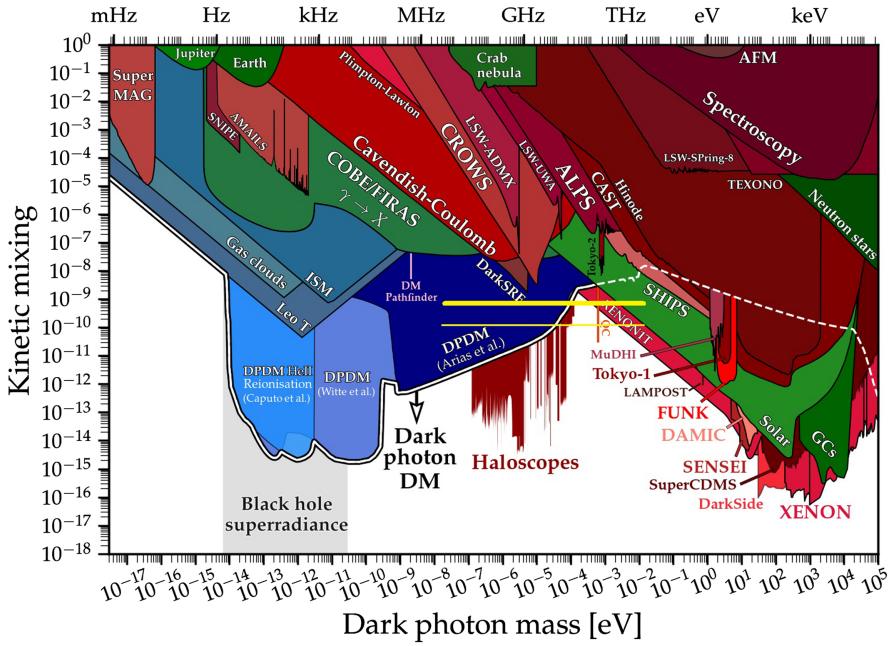

FIG. 2. The expected constrained of the discussed technique on the kinetic mixing α is marked on the standard diagram [71] by the yellow solid lines. Thick line is for the conservative and thin one for the optimistic sensitivity estimate as discussed in the text. In both cases the proposed technique allows for partial filling of the gap between haloscopes' and XENON1T's measurements.

amplitude by stochastic component means that the field reads $\mathbf{E}(\mathbf{r},t) = \mathrm{Re}[\mathbf{E}_0 e^{i(\mathbf{kr}-\omega t)} + \frac{\Delta\mathbf{E}_0}{2}(e^{i((\mathbf{k}-\mathbf{k}_0)\mathbf{r}-(\omega-\omega_0)t)} + e^{i((\mathbf{k}+\mathbf{k}_0)\mathbf{r}-(\omega+\omega_0)t)})]$. Here, k_0, ω_0 is the wave vector and frequency of the amplitude modulations. In principle, all involved phases can be shifted by arbitrary constants, but we neglect here such phase shifts for simplicity. In analogy to the calculations in Sec. VI we propagate all components of the field with fluctuating amplitude and get at $\mathbf{r} = 0$

$$\mathbf{E}_{\mathrm{tot}}(t) = \mathrm{Re}\left[\mathbf{E}_0 B(\omega) e^{-i(\omega t+\phi)} + \frac{\Delta\mathbf{E}_0}{2} B(\omega_-) e^{-i(\omega_- t+\phi_-)} + \frac{\Delta\mathbf{E}_0}{2} B(\omega_+) e^{-i(\omega_+ t+\phi_+)}\right]. \tag{52}$$

We reintroduced arbitrary phases ϕ and ϕ_0 and denoted $\phi_\pm = \phi \pm \phi_0$, $\omega_\pm = \omega \pm \omega_0$. The function $B(\omega) = \frac{e^{i\frac{\omega L}{2c}}}{1+re^{i\frac{\omega L}{c}}}$ is the same enhancement factor as in the relation (50).

To be on the save side one should take into account the enhanced fields at the minimum and enhanced noise at the maximal values. This leads to the conservative estimation. The order of the magnitude calculation of the accuracy, using the parameters relevant for our proposal of the same value as in [69], leads to a rough sensitivity estimation of the order of $\alpha \approx 10^{-10} \div 10^{-9}$. Importantly, even with the conservative estimate the technique may be of importance, as it fills the gap between the existing measurements by XENON1T and haloscope experiments as visible from the Fig. 2. In the figure the thick-yellow horizontal line shows the limit of the kinetic mixing corresponding to our sensitivity estimate $= 10^{-9}$. The expected increase of sensitivity to 10^{-10} due to correlation between two signals at two frequencies further closes the existing gap. This is represented by the thin yellow line in the figure.

We now provide a discussion of the experimental setup and the mass range which can be accessed by the present technique. The measurements of ac longitudinal and anomalous Hall currents are among standard tools in the condensed matter field. The limitation on the upper limit of the dark photon mass is related to its expected de Broglie wavelength $\lambda_{\mathrm{DP}} = \frac{h}{m_{\mathrm{DP}} v_{\mathrm{DP}}}$, which should be greater than the typical size of the measured sample L_s. Using $L_s \approx 1$ mm–1 cm, $v_{\mathrm{DP}} \approx 10^{-3}c$ one gets the upper-mass limit ≈6–60 meV. Knowing the dark matter density ρ and assuming that it is composed of dark photons of the above mass only we estimate that there exist about 10^{11}–10^{10} of them in each cubic cm of space around Earth.

The limit on the lower mass range depends on the particular detection scheme. We discuss here the most promising scheme requiring simultaneous measurements of nonlinear anomalous Hall currents at two frequencies $\omega \pm \tilde{\omega}$, distance $2\tilde{\omega}$ apart. If the frequency $\tilde{\omega}$ is too small the total frequency shift $2\tilde{\omega}$ may not exceed the width of the experimental signal peak making the frequency shift unobservable. Even though the precise numbers do depend on experimental setup we expect that other unexplored mass range, namely $m_{\mathrm{DP}} < 10^{-14}$ eV [cf. wide unexplored range of masses in Fig. 2], is not accessible in the current scheme.

By definition the observed currents do not depend on the mass of the sample or the acquisition time. Moreover, the sensitivity estimate does not depend on the mass/frequency range and is thus valid from the lowest (in actual experimental practice of an order of hundred Hz) up to THz frequencies.

Additionally to the above estimates on the sensitivity we propose another piece of information related to the issue and a particular technique of measuring the anomalous Hall current. One way to learn about the high-frequency anomalous Hall conductance of materials is to measure the change of the angle between the beams of linearly polarized light incident and reflected from the surface of material displaying the Hall effect [72]. This technique known as Kerr effect has been widely utilized in measuring the Hall effect in superconductors with time-reversal breaking order parameter [73] without external magnetic field. To measure the tiny effects in Sr_2RuO_4 [74] and other superconductors special instrument was built [75] reaching the accuracy of Kerr angle measurements as small as a few nrad at energy of light quanta $= 0.8$ eV. Combining this with recent calculations [76] which show that in Weyl semimetals the Kerr angle is of order of 0.1 rad one gets the realistic estimate of sensitivity for the existing apparatus and typical materials of the order of 10^{-8}. We propose to measure three different signals, so the statistical correlations among them can be utilized to identify the events even if the individual measurements are less precise.

VIII. DISCUSSION OF DETECTION SCENARIOS AND CONCLUSIONS

We consider massive dark photon as a source of the electric field which couples to the standard one by kinetic mixing characterized by the coupling α. With both, Maxwell and dark photon fields of respective frequencies ω and $\tilde{\omega}$ taken into account, we have solved the Boltzmann equation up to the first order in the fields, although, the proposed scheme is valid to all orders. Moreover, the closed non-perturbative solution (valid to an arbitrary order of the electric fields) can also be obtained by straightforward generalization of the recent paper [60]. The alternating longitudinal and anomalous Hall currents induced by the sum of the external electric field and the field due to the dark photon are calculated up to the second order in the fields and up to the linear order in the coupling α. There are three contributions of order of α^1. The conservative estimations show the sensitivity which sets the limit about 10^{-9}–10^{-10}. The proposed experiments may fill the gap between the XENON1T and haloscope measurements, as visible from Fig. 2. The existing instrumentation should potentially allow the detection of the effect in Weyl semimetals.

Various detecting scenarios can be thought about in the context of the present proposal. Nevertheless, one has to recall that the α-coupling constant in the kinetic mixing term is expected to be small, $\alpha \ll 1$, so the terms of order α^2 can be probably neglected as unmeasurable, even with application of resonant electromagnetic cavities. This is true for the second term of the rectified current (30) and for the current (34) which is also proportional to $\alpha^2 \tilde{\mathbf{E}}^2_{(0)}$.

The expectation is that some of the two dimensional transition metal dichalcogenides or other materials [77] with nonvanishing Berry curvature could serve the purpose. These materials are relatively clean and their two-dimensional character make the high-frequency transport measurements easier than their three-dimensional counterparts. The expectation that the two-dimensional system may in some cases be better probes comes from the observation that, e.g., in graphene a very large nonlinear Kerr effect [78] has been measured. However, not the dimensionality itself, but the distance Δk_W between the Weyl nodes seems to be the most important parameter, as the recent calculations suggest [76], because the Kerr signal is directly proportional to it.

We mention here the most obvious scenarios, leaving more detailed analysis to the future work. One can imagine (i) measuring the current (28), which is the ac analog of the anomalous Hall [79] current in the topological material with broken time-reversal symmetry. In a similar manner (ii) the longitudinal current given by (32) is linear in $\tilde{\mathbf{E}}_{(0)}$. This current can also be spotted in a standard metallic system without Berry curvature. Both these currents appear when the dark particle occasionally collides with the studied material and produces oscillating electric field $\propto \alpha \tilde{\mathbf{E}}(t)$ in the absence of external standard electric field $\mathbf{E} = 0$.

Scenario (iii) relies on the application of a strong ac standard electric field $\mathbf{E}$ of frequency ω and studying longitudinal and Hall currents at frequencies $\omega \pm \tilde{\omega}$. This is potentially very precise measurement which, however, requires the knowledge of frequency $\tilde{\omega}$ [80]. Unfortunately, the dark field frequency is unknown and thus the apparatus and measurement details have to be tuned for each expected mass, in a way very much similar as in other existing or proposed experiments.

Surely, the simultaneous observation of all three currents is potentially the most desired scenario. The rough estimations suggest that the technique sensitivity could be better than 10^{-10}, especially if the temporal correlations among three different signals are utilized.

Our proposal supplements other techniques based on the condensed matter systems. The important aspect of the present proposal is the possibility to measure essentially simultaneously a few currents using topological quantum materials (with Berry curvature). One expects the existence of three signals with one longitudinal and two ac anomalous Hall currents. They appear at a few frequencies, e.g., $\tilde{\omega}, \omega \pm \tilde{\omega}$, which provides additional control on the effect and an additional experimental knob, which can be effectively used to identify the mass of the dark photon.

In summary, we have proposed to search for the dark matter induced electric fields by means of the transport currents in chiral Weyl or Dirac semimetals. The discussed here detection scheme of the dark matter is based on the observations of ac longitudinal and Hall currents.

ACKNOWLEDGMENTS

K. I. W. and M. R. were partially supported by Grant No. 2022/45/B/ST2/00013 of the National Science Center, Poland.

[1] G. Bertone and D. Hoope, History of dark matter, Rev. Mod. Phys. **90**, 507 (2018).
[2] C. S. Frenk and S. D. M. White, Dark matter and cosmic structure, Ann. Phys. (Berlin) **524**, 507 (2012).
[3] J. M. Gaskins, A review of indirect searches for particle dark matter, Contemp. Phys. **57**, 496 (2016).
[4] S. Bird, I. Cholis, J. B. Muñoz, Y. Ali-Haïmoud, M. Kamionkowski, E. D. Kovetz, A. Raccanelli, and A. G. Riess, Did LIGO detect dark matter?, Phys. Rev. Lett. **116**, 201301 (2016).
[5] G. Bertone and T. M. P. Tait, A new era in the search for dark matter, Nature (London) **562**, 52 (2016).
[6] M. Battaglieri, A. Belloni, A. Chou *et al.*, US Cosmic Visions: New ideas in dark matter 2017: Community Report, arXiv:1707.04591v1.
[7] K. A. Meissner and H. Nicolai, Planck mass charged gravitino dark matter, Phys. Rev. D **100**, 035001 (2019).
[8] D. Kim, J.-C. Park, K. C. Fong, and G.-H. Lee, Detection of super-light dark matter using graphene sensor, arXiv:2002.07821v3.
[9] A. V. Dixit, S. Chakram, K. He, A. Agrawal, R. K. Naik, D. I. Schuster, and A. Chou, Searching for dark matter with a superconducting qubit, Phys. Rev. Lett. **126**, 141302 (2021).
[10] M. Rogatko and K. I. Wysokiński, Chiral kinetic theory in the presence of dark photon, Phys. Rev. D **107**, 044036 (2023).
[11] D. K. Hong, S. H. Im, K. S. Jeong, and D.-h. Yeom, Detecting axion dark matter with chiral magnetic effects, arXiv:2207.06884.
[12] Y. Hochberg, B. V. Lehmann, I. Charaev, J. Chiles, M. Colangelo, S. W. Nam, and K. K. Berggren, New constraints on dark matter from superconducting nanowires, Phys. Rev. D **106**, 112005 (2022).
[13] S. Knapen, J. Kozaczuk, and T. Lin, Migdal effect in semiconductors, Phys. Rev. Lett. **127**, 081805 (2021).
[14] Z.-L. Liang, C. Mo, F. Zheng, and P. Zhang, Phonon-mediated Migdal effect in semiconductor detectors, Phys. Rev. D **106**, 043004 (2022).
[15] H.-Y. Chen, A. Mitridate, T. Trickle, Z. Zhang, M. Bernardi, and K. M. Zurek, Dark matter direct detection in materials with spin-orbit coupling, Phys. Rev. D **106**, 015024 (2022).
[16] I. M. Bloch, G. Ronen, R. Shaham, O. Katz, T. Volansky, and O. Katz, New constraints on axion-like dark matter using a Floquet quantum detector, Sci. Adv. **8**, eabl8919 (2022).
[17] Y. Hochberg, T. Lin, and K. M. Zurek, Detecting ultralight bosonic dark matter via absorption in superconductors, Phys. Rev. D **94**, 015019 (2016).
[18] S. Knapen, T. Lin, and K. M. Zurek, Light dark matter in superfluid helium: Detection with multi-excitation production, Phys. Rev. D **95**, 056019 (2017).
[19] S. Knapen, T. Lin, M. Pyle, and K. M. Zurek, Detection of light dark matter with optical phonons in polar materials, Phys. Lett. B **785**, 386 (2018).
[20] R. Budnik, O. Cheshnovsky, O. Slone, and T. Volansky, Direct detection of light dark matter and solar neutrinos via color center production in crystals, Phys. Lett. B **782**, 242 (2018).
[21] Y. Hochberg, Y. Kahn, M. Lisanti, K. M. Zurek, A. G. Grushin, R. Ilan, S. M. Griffin, Z-F. Liu, S. F. Weber, and J. B. Neaton, Detection of sub-MeV dark matter with three-dimensional Dirac materials, Phys. Rev. D **97**, 015004 (2018).
[22] T. Liang, B. Zhu, R. Ding, and T. Li, Direct detection of axion-like particles in Bismuth-based topological insulators, Int. J. Mod. Phys. A **33**, 1850135 (2018).
[23] M. Baryakhtar, J. Huang, and R. Lasenby, Axion and hidden photon dark matter detection with multilayer optical haloscopes, Phys. Rev. D **98**, 035006 (2018).
[24] M. Rogatko and K. I. Wysokiński, P-wave holographic superconductor/insulator phase transitions affected by dark matter sector, J. High Energy Phys. 03 (2016) 215.
[25] M. Rogatko and K. I. Wysokiński, Holographic vortices in the presence of dark matter sector, J. High Energy Phys. 12 (2015) 041.
[26] M. Rogatko and K. I. Wysokiński, Condensate flow in holographic models in the presence of dark matter, J. High Energy Phys. 10 (2016) 152.
[27] M. Rogatko and K. I. Wysokiński, Viscosity bound for anisotropic superfluids with dark matter sector, Phys. Rev. D **96**, 026015 (2017).
[28] B. Kiczek, M. Rogatko, and K. I. Wysokiński, Holographic DC SQUID in the presence of dark matter, J. Cosmol. Astropart. Phys. 01 (2021) 063.
[29] Y. Kahn and T. Lin, Searches for light dark matter using condensed matter systems, Rep. Prog. Phys. **85**, 066901 (2022).
[30] A. Mitridate, T. Trickle, Z. Zhang, and K. M. Zurek, Snowmass white paper: Light dark matter direct detection at the interface with condensed matter physics, Phys. Dark Universe **40**, 101221 (2023).

[31] B. Holdom, Two $U(1)$'s and epsilon charge shifts, Phys. Lett. **166B**, 196 (1986).
[32] A. Caputo, A. J. Millar, C. A. J. O'Hare, and E. Vitagliano, Dark photon limits: A handbook, Phys. Rev. D **104**, 095029 (2021).
[33] B. S. Acharya, S. A. R. Ellis, G. L. Kane, B. D. Nelson, and M. J. Perry, Lightest Visible-sector supersymmetric particle is likely unstable, Phys. Rev. Lett. **117**, 181802 (2016).
[34] S. A. Abel and B. W. Schofield, Brane-antibrane kinetic mixing, millicharged particles and SUSY breaking, Nucl. Phys. **B**, 685, 150 (2004).
[35] S. A. Abel, J. Jaeckel, V. V. Khoze, and A. Ringwald, Illuminating the hidden sector of string theory by shining light through a magnetic field, Phys. Lett. B **666**, 66 (2008).
[36] S. A. Abel, M. D. Goodsell, J. Jaeckel, V. V. Khoze, and A. Ringwald, Kinetic mixing of the photon with hidden U(1)s in string phenomenology, J. High Energy Phys. 07 (2008) 124.
[37] K. Van Tilburg, N. Leefer, L. Bougas, and D. Budker, Search for ultralight scalar dark matter with atomic spectroscopy, Phys. Rev. Lett. **115**, 011802 (2015).
[38] J. H. Chang, R. Essig, and S. D. McDermott, Revisiting Supernova 1987A constraints on dark photons, J. High Energy Phys. 01 (2017) 107.
[39] M. Crisler *et al.* (SENSEI Collaboration), SENSEI: First direct-detection constraints on sub-GeV dark matter from a surface run, Phys. Rev. Lett. **121**, 061803 (2019).
[40] J. P. Lees *et al.*, Search for a dark photon in e^+e^- collisions at *BABAR*, Phys. Rev. Lett. **113**, 201801 (2014).
[41] A. W. Thomas, X. G. Wang, and A. G. Williams, Sensitivity of parity-violating scattering to dark photon, Phys. Rev. Lett. **129**, 011807 (2022).
[42] H. An, S. Ge, W-Q. Guo, X. Huang, J. Liu, and Z. Lu, Direct detection of dark photon dark matter using radio telescopes, Phys. Rev. Lett. **130**, 181001 (2023).
[43] P. Jean *et al.*, Early SPI/INTEGRAL measurements of 511 keV line emission from the 4th quadrant of the galaxy, Astron. Astrophys. **407**, L55 (2003).
[44] J. Chang *et al.*, An excess of cosmic ray electrons at energies of 300–800 GeV, Nature (London) **456**, 362 (2008).
[45] E. Bulbul, M. Markevitch, A. Foster, R. K. Smith, M. Loewenstein, and S. W. Randall, Detection of an unidentified emission line in the stacked X-ray spectrum of galaxy clusters, Astrophys. J. **789**, 13 (2014).
[46] A. Geringer-Sameth and M. G. Walker, Indication of gamma-ray emission from the newly discovered dwarf galaxy reticulum II, Phys. Rev. Lett. **115**, 081101 (2015).
[47] K. K. Boddy and J. Kumar, Indirect detection of dark matter using MeV-range gamma-rays telescopes, Phys. Rev. D **92**, 023533 (2015).
[48] M. Fabbrichesi, E. Gabrielli, and G. Lanfranchi, *The Physics of the Dark Photon* (Springer, New York, 2021).
[49] A. Iwazaki, A new method for detecting axion with cylindrical superconductor, Phys. Lett. B **811**, 135861 (2020).
[50] A Iwazaki, Axion-radiation conversion by super and normal conductors, Nucl. Phys. **B**, 963, 115298 (2021).
[51] Y. Kishimoto and K. Nakayama, Electric current on surface of a metal/superconductor in axion/hidden-photon background, Phys. Lett. B **827**, 13 (2022).
[52] N. P. Armitage, E. J. Mele, and A. Vishwanath, Weyl and Dirac semimetals in three-dimensional solids, Rev. Mod. Phys. **90**, 015001 (2018).
[53] B. Q. Lv, T. Qian, and H. Ding, Experimental perspective on three-dimensional topological semimetals, Rev. Mod. Phys. **93**, 025002 (2021).
[54] I. Sodemann and L. Fu, Quantum nonlinear Hall effect induced by Berry curvature dipol in time-reversal invariant materials, Phys. Rev. Lett. **115**, 216806 (2015).
[55] G. Wang, A. Chernikov, M. M. Glazov, T. F. Heinz, X. Marie, T. Amand, and B. Urbaszek, Colloquium: Excitons in atomically thin transition metal dichalcogenides, Rev. Mod. Phys. **90**, 021001 (2018).
[56] Cui-Zu Chang, Chao-Xing Liu, and Allan H. MacDonald, Colloquium: Quantum anomalous Hall effect, Rev. Mod. Phys. **95**, 011002 (2023).
[57] Di Xiao, M.-C. Chang, and Q. Niu, Berry phase effect on electronic properties, Rev. Mod. Phys. **82**, 1959 (2010).
[58] G. D. Mahan, *Many-Particle Physics*, 3rd ed. (Kluwer Academic/Plenum Publishers, New York, 2000).
[59] D. T. Son and B. Z. Spivak, Chiral anomaly and classical negative magnetoresistance of Weyl metals, Phys. Rev. B **88**, 104412 (2013).
[60] R. M. A. Dantas, Z. Wang, P. Surówka, and T. Oka, Nonperturbative topological current in Weyl and Dirac semimetals in laser fields, Phys. Rev. B **103**, L20115 (2021).
[61] Z.-F. Zhang, Z.-G. Zhu, and G. Su, Theory of nonlinear response for charge and spin currents, Phys. Rev. B **104**, 115140 (2021).
[62] Z.-Y. Zhuang and Z. Yan, Extrinsic and intrinsic nonlinear Hall effects across Berry-dipole transitions, Phys. Rev. B **107**, L161102 (2023).
[63] C.-P. Zhang, X.-J. Gao, Y.-M. Xie, H. C. Po, and K. T. Law, Higher-order nonlinear anomalous Hall effects induced by Berry curvature multipoles, Phys. Rev. B **107**, 115142 (2023).
[64] L. Xiang, C. Zhang, L. Wang, and J. Wang, Third-order intrinsic anomalous Hall effect with generalized semiclassical theory, Phys. Rev. B **107**, 075411 (2023).
[65] R. Guo, C. Liu, S. Mao, X. Xue, R. J. Long, and L. Zhang, Measuring the local dark matter density with LAMOST DR5 and Gaia DR2, Mon. Not. R. Astron. Soc. **495**, 4828 (2020).
[66] A. Loeb, New way to limit the interaction of dark matter with baryons, Phys. Rev. D **105**, L0911903 (2022).
[67] A. Amruth, T. Broadhurst, J. Lim, M. Oguri, G. F. Smoot, J. M. Diego, E. Leung, R. Emami, J. Li, T. Chiueh, H.-Y. Schive, M. C. H. Yeung, and S. K. Li, Einstein rings modulated by wavelike dark matter from anomalies in gravitationally lensed images, Nat Astron **7**, 736 (2023).
[68] J. Beringer *et al.*, Review of particle physics, Phys. Rev. D **86**, 01001 (2012).
[69] J. Gue, A. Hees, J. Lodewyck, R. Le Targat, and P. Wolf, Search for vector dark matter in microwave cavities with Rydberg atoms, Phys. Rev. D **108**, 035042 (2023).
[70] David A. Hill, *Electromagnetic Fields in Cavities: Deterministic and Statistical Theories*, (Institute of Electrical and Electronics Engineers Press, John Wiley and Sons, Inc., Hoboken, New Jersey, 2009).
[71] See: https://cajohare.github.io/AxionLimits/docs/dp.html.

[72] R. Shimano, Y. Ino, Yu. P. Svirko, and M. Kuwata-Gonokami, Terahertz frequency Hall measurement by magneto-optical Kerr spectroscopy in InAs, Appl. Phys. Lett. **81**, 199 (2002).

[73] A. Kapitulnik, J. Xia, E. Schemm, and A. Palevski, Polar Kerr effect as probe for time-reversal symmetry breaking in unconventional superconductors, New J. Phys. **11**, 055060 (2009).

[74] K. I. Wysokiński, James F. Annett, and B. L. Györffy, Intrinsic optical dichroism in the chiral superconducting state of Sr2RuO4, Phys. Rev. Lett. **108**, 077004 (2012); **108**, 077004 (2012).

[75] J. Xia, P. T. Beyersdorf, M. M. Fejer, and A. Kapitulnik, Modified Sagnac interferometer for high-sensitivity magneto-optic measurements at cryogenic temperatures, Appl. Phys. Lett. **89**, 062508 (2006).

[76] K. Sonowal, A. Singh, and A. Agarwal, Giant optical activity and Kerr effect in type-I and type-II Weyl semimetals, Phys. Rev. B **100**, 085436 (2019).

[77] A. V. Pronin and M. Dressel, Nodal semimetals: A survey on optical conductivity, Phys. Status Solidi B **258**, 2000027 (2021).

[78] H. Zhang, S. Virally, Q. Bao, K. P. Loh, S. Massar, N. Godbout, and P. Kockaert, Large nonlinear Kerr effect in graphene, Opt. Lett. **37**, 1858 (2012).

[79] F. D. M. Haldane, Berry curvature on the Fermi surface: Anomalous Hall effect as a topological Fermi-liquid property, Phys. Rev. Lett. **93**, 206602 (2004).

[80] A. Zong, B. R. Nebgen, S.-C. Lin, J. A. Spies, and M. Zuerch, Emerging ultrafast techniques for studying quantum materials, Nat. Rev. Mater. **8**, 224 (2023).